THE IMPACT OF THE SUMMIT STATION, GREENLAND RADIOSONDE PROGRAM ON WEATHER AND CLIMATE PREDICTION

An Undergraduate Research Scholars Thesis

by

CARLOS MARTINEZ

Submitted to the Undergraduate Research Scholars program
Texas A&M University
in partial fulfillment of the requirements for the designation as an

UNDERGRADUATE RESEARCH SCHOLAR

Approved by
Research Advisor: Dr. Oliver Frauenfeld

May 2016

Major: Meteorology

TABLE OF CONTENTS

ABSTRACT

The Impact of the Summit Station, Greenland Radiosonde Program on
Weather and Climate Prediction

Carlos Martinez
Department of Atmospheric Science
Texas A&M University

Research Advisor: Dr. Oliver Frauenfeld
Department of Geography

Radiosonde data from weather balloons are critical because they are essential inputs for numerical weather prediction models and are used for climate research. However, radiosonde programs are costly to maintain, in particular in the remote regions of the Arctic. The climate of this data-sparse region is poorly understood and forecast data assimilation procedures are designed for more general, global applications. Thus, observations may be rejected from the data assimilation because they are too far from the forecast model expectations. Here, we evaluate how radiosondes launched twice daily (0 and 12 UTC) from Summit Station, Greenland, (72.58°N, 38.48°W, 3210 masl) influence the European Centre for Medium Range Weather Forecasting (ECMWF) operational forecasts from June 2013 through May of 2015. Several stakeholders use this information for forecasting and research, such as investigating the changing climate, including that of the Greenland Ice Sheet (GIS). Therefore, a statistical analysis is conducted to determine the impact of these radiosonde observations on the forecast model, and the meteorological regimes that the model fails to reproduce will be identified. First, the frequency of the deployment of radiosondes is calculated, and approximately 90% or more of the deployments were successful. Next, the climatology of the GIS temperature inversions is calculated, and it is found that ECMWF underestimates temperature inversions. The assimilation rates of meteorological variables that influence the variability of the inversion strength –

temperature, specific humidity, are lowest in the layer where the inversion strength is located. Therefore, there is a likely relationship between model simulations with and without these meteorological variables assimilated, and the underestimation of this particular meteorological regime. Meanwhile, winds – another influence on the variability of temperature inversion – had high assimilation rates, likely caused by being the only observational source for the model. Based on a statistical assessment, the magnitude of the mean model bias for simulations without temperature and specific humidity data assimilated is significantly reduced in comparison model with radiosonde observations assimilated. Overall, the radiosonde data provided by the Summit Station radiosonde program improves meteorological forecasts in ECMWF. This likely improves the underestimation of surface features on the GIS, such as shallow temperature inversions, which leads to improved understanding of the climatic and atmospheric dynamics of the GIS.

ACKNOWLEDGMENTS

I would first like to thank Dr. Frauenfeld for his tremendous guidance and assistantship as a mentor throughout the entire year with this project. I would also like to thank the Undergraduate Research Scholars Program for their assistantship with the formatting of the Thesis, in addition to their guidance throughout the submittal process. To Sandy Starkweather and the mentorship team: Christopher Cox, Matt Shupe, and Amy Solomon when this project started through the National Oceanic and Atmospheric Administration Hollings Scholarship Program. To the ECMWF community, specifically, Ersagun Kuscu and Thomas Haiden for providing the ECMWF dataset. To Ann Thorne, coordinator of student programs at the Earth System Research Laboratory, and the NOAA Office of Education and Student Scholarship Team for the NOAA Hollings Internship Program.

CHAPTER I

INTRODUCTION

Earth's North Polar Region

The Arctic is Earth's polar region of the northern hemisphere encompassing the Arctic Ocean and major land masses such as Greenland, Siberia, and most northern parts of North America and Europe. Above 66.5°N latitude, the polar region is defined for its contrasts in daylight by season, where there is little to no sunlight late fall into winter, and complete daylight throughout the entire summer until early fall.

The main and most distinctive feature of the Arctic is its ice cover. The Arctic ice cap encompasses a majority of the Arctic Ocean and some Arctic land masses. The ice sheet undergoes a seasonal cycle where its surface area thickness is at a minimum by mid-September due to melting, and peaks by mid-March. Sea ice is a significant feature of the Arctic and dictates the climatology of the Arctic Circle. Ice in general has a high albedo, meaning it reflects most of the incoming solar radiation. This has a profound effect on the surface heat exchange in the Arctic. Unlike the GIS, sea ice is much thinner and is therefore more sensitive to small changes in heat input (Maykut 1986). In addition, ice affects the vertical mixing in the oceans because the formation of ice causes salt to be removed from the near-surface layer of the ocean. The denser surface water, due to the higher salinity sinks, causes circulation overturning. This process is important in the development of the North Atlantic Deep Water (NADW), a major oceanic feature that circulates southern hemisphere warm waters into the North Atlantic.

Arctic Temperature Inversions

An important and distinctive feature in the Arctic is a low-level temperature inversion. In the Mid-Latitudes and Tropics, typically the air temperature decreases with height. However, in the Arctic, temperature frequently increases with height due to the ice cover and its reflective properties of incoming radiation (Miller et al. 2013). The surface therefore experiences cooling, and the shallow layer of air above it is relatively warmer. Other atmospheric conditions such as warm air advection, subsidence, surface melt, and topography all contribute to the extent of the shallow temperature inversions across the Arctic. Typically, in the Arctic, inversions are stronger during the winter months, and weaker during the summer time. However, summer temperature inversions are also frequently observed, and contribute to surface melting of ice.

Temperature inversions are essential for determining snowfall, glacier mass, and ice melt estimations across the Arctic (Mernild and Liston 2010). These Arctic temperature inversions are frequently present on local and regional scales, where their strength and seasonality plays an important role on the climatology of the Arctic. However, the complexities of this phenomenon are an area of active research. The logistical constraints and harsh climate in remote regions of the Arctic make capturing and simulating Arctic temperature inversions extremely difficult.

Climate Change in the Arctic

The Arctic system has been rapidly changing due to climate change. The altering surface composition in high northern latitudes, snow and ice, the stability of the lower troposphere, and degradation of permafrost are some of several important responses from current anthropogenic greenhouse warming. Of all climate regions on Earth, the Arctic continues to experience the largest mean annual surface air temperature increases. From satellite measurements and surface observations, a decrease in sea ice extent across the Arctic Circle is evident (Serreze et al. 2001). Furthermore, an ecological response is occurring: there is evidence of a northward migration in the tree line, and an increase in plant growth in regions typically barren or associated with snow cover (Serreze et al. 2001). Changing weather conditions and ice dynamics are pose increasing difficulties for land- and marine- based transportation, and opening uncharted political waters for economic investments (Ford et al. 2014). The extent to which the Arctic climate is changing from anthropogenic drivers, however, is to this date an ongoing debate. Natural interdecadal variabilities of large atmospheric features such as the Southern Oscillation, the North Atlantic Oscillation and its hemispheric counterpart, the Arctic Oscillation, all play influential roles. However, as found in Overpeck et al. (1997), the temperature record in the Arctic suggest it is the warmest it has been in the past 400 years. Furthermore, there are other variables from climate change that are affecting the amplified warming of the Arctic. For instance, baroclinic weather systems in the North Atlantic and associated mid-latitude changes are a significant cause of an increase in northward heat and moisture transport from the Tropics to the Arctic (Graversen et al. 2006). This external forcing is a likely contributor to the observed temperature amplification and warming of the vertical structure of the Arctic (Graversen et al. 2006).

Given the dynamic, harsh, and sparsely vegetated system that is the Arctic, integrated studies regarding the climate of the Arctic is relatively new. For instance, the complexity of surface runoff is caused by the unknown magnitude of declines in glaciers and permafrost in a given region (Hinzmann et al. 2005). Given a potential increase in vegetation, increased precipitation may be counterbalanced by an increase in evapotranspiration. These uncertainties, in addition to the ongoing human component of the system, are critically important topics. Therefore, the ability to observe the dynamical links associated with the changing climate of the Arctic is important. For example, understanding the temperature and precipitation variability in certain areas of the Arctic is essential to understanding the spatial and temporal changes occurring in the overall region. A region of particular interest is Greenland and its influential role in affecting the overall climate of the Arctic.

The Greenland Ice Sheet

Greenland is the largest island in the world, surrounded by the Arctic and North Atlantic Oceans, and encompasses a major portion of the Arctic. With a size of 2,166,086 km^2, Greenland stretches from approximately 59N to 83N, a distance from point to point of nearly 2,650,000 m, and longitudinally from 11W to 72W. The average elevation of Greenland is approximately 3,700 meters, but varies season to season due to fluctuations in ice gain and melt. The area of the ice sheet is approximately 1.71×10^6 km^2 and the area of glaciers and ice caps are approximately 0.05×10^6 km^2 (Weidick 1995). Mean temperatures across Greenland vary from its western and eastern regions. The annual range of monthly mean temperatures is between 23.5°C and 30.3°C for the western region of the ice sheet, with a gradient of -0.78°C/1° latitude (Box and Steffen 2001). The eastern side of Greenland is slightly colder, with a gradient of -0.82°C/1° latitude (Box and Steffen 2001). In addition, a prominent atmospheric feature exists on the Greenland GIS: a shallow, surface-based temperature inversion. Rapid cooling of the ice surface, typically during clear-sky conditions (Miller et al. 2013), causes a shallow temperature inversion, varying from season to season. Temperature inversions in Greenland are important for understanding the climatological processes of the GIS, such as energy and mass exchanges between the surface and overlying atmosphere.

Changes in Greenland from Arctic Warming

Changes in the dynamics and physical structure of Greenland due to enhanced warming in the Arctic are a great concern as these changes can alter the Arctic and North Atlantic climate. Satellite measurements have shown positive trends in temperatures over the past decade in parts of the GIS (Hall et al. 2013). Several global and regional model simulations indicate a warming trend in the Arctic throughout the 21st Century. Particularly in Greenland, the melting of the GIS due to this warming has important ramifications. From 1992 to 2011, approximately 2700 ± 930 Gt of ice was lost from the ice sheets of Greenland, corresponding to a global mean sea level rise of 11.2 ± 3.8 mm (Shepherd et al. 2012). During the summer, glacial meltwater bodies, such as ponds and lakes, develop across the GIS. These bodies leave drainage flows beneath the GIS that rapidly enter the ocean basins. With warming, these lakes are predicted to increase in size and number. Observational studies regarding these surface water bodies and their drainage systems have determined that the ice sheet drains under these conditions and thus the prediction of the flow by models is difficult due to the unknown subglacial processes associated with the GIS (Smith et al. 2014). Numerous assessments such as from the Intergovernmental Panel on Climate Change, suggest a 0.02 to 0.09 m increase in global sea level rise by the end of the 21st Century from the GIS (Church et al. 2013). In addition, the decline in the GIS causes an increase in freshwater flux into the North Atlantic (Fichefet et al. 2003). In response, the thermohaline circulation of the NADW is suppressed, causing regional climactic effects across the North Atlantic.

Observational Network System in Arctic

Given the harsh climate and lack of accessibility of the Arctic, the installation of atmospheric observing stations and collection of atmospheric measurements with consistency is very challenging. In addition, any past measurements made in the Arctic were short-lived, mainly due to independent experimentation conducted by scientists for their own short-termed studies. Satellite measurements are useful, but have their own shortcomings due to the obstruction of clouds. These challenges affect the quality of meteorological and climatological Arctic forecasts provided by numerical models. Numerical models make predictions of future weather and climate conditions provided by past and present data. Essential for understanding the future of a given region, the lack of observational data in the Arctic for driving models is a cause for concern when investigating the Arctic's changing dynamics. In addition, numerical models sometimes falsely reject the observational information because the values – while real – may seem too extreme. Therefore, in the early 2010s, the International Arctic Systems for Observing the Atmosphere was initiated as an International Polar Year project (Darby et al. 2011) to investigate many of the outstanding questions through coordinating the considerable atmospheric observing assets at several Arctic stations (Sandy et al. 2013). The program has been able to install and maintain instruments for long durations, thereby enhancing the understanding and forecasting of the Arctic. An important observational tool, which this network and several institutions rely on are radiosondes. Radiosondes are balloon-borne meteorological sensors used to acquire atmospheric profiles of variables including temperature and humidity and thus are significant observational tools for weather forecasting and climate science. In the entire Arctic however, only 40 (out of approximately 1000) routine global launches are made, leaving a potentially large gap in the understanding of the atmosphere. With the numerous economic and political ventures associated with this poorly understood region, an assessment of the value of the current radiosonde programs is necessary. In Greenland, Summit Station is the only radiosonde site within the entire 2.2 million km^2 mainland of Greenland, and is costly to maintain at $440,000 per year. The vertical temperature profiles provided by radiosondes are crucial for properly capturing atmospheric features such as the surface-based temperature inversion. Furthermore, it is important to evaluate the degree to which forecast models can properly capture this shallow and unique feature when radiosondes are assimilated into the model. Greenland's unique atmospheric conditions and significant climatological effects on the entire Arctic motivate this study, which will analyze how well the radiosonde program captures these distinct features and how the information is beneficial for the scientific community.

Objectives and Goals

For the most cost-effective deployment of resources and to improve forecasting methods, analyses of the effectiveness of individual radiosonde programs are necessary. Our goal is to evaluate how radiosondes launched twice daily, at 0 and 12 UTC, from Summit Station, Greenland (72.58°N, 38.48°W, 3210 masl), influence the European Centre for Medium Range Weather Forecasting (ECMWF) operational forecasts. The evaluation consists of three main objectives. The first is to assess the radiosonde assimilation rates by the ECMWF model under varying meteorological conditions. Specifically, I will identify the meteorological regimes that result in lower assimilation. Given the GIS's shallow inversion and unexpected temperature profile, assimilation rates are likely to be lower in the lower levels of the atmosphere than the upper-levels. Next, I will quantify the improvement in model forecasts when radiosonde data end up getting assimilated. Depending on the assimilation rates, a positive influence is likely, given the assumption that computer models could otherwise not capture the temperature inversion on the GIS. Finally, I will assess the connection between accurately characterizing the atmosphere over Greenland and weather prediction and climate in the region. A better understanding of the atmospheric phenomena on Greenland, such as the temperature inversion but also other synoptic meteorological conditions can further advance weather forecasting and climate science in the Arctic.

CHAPTER II

DATA

Summit Station Radiosonde Data

The Summit Station program (Shupe et al. 2013) launches radiosonde instruments twice a day at approximately 0 UTC and 12 UTC (72.58°N, 38.48°W, 3210 masl). The radiosonde program began in May of 2010 and is ongoing only until 2017, unless continued via additional funding. The data are available from both the U.S. Department of Energy Atmospheric Radiation Measurement, and from the NOAA Earth System Research Laboratory. The dataset used for the project ranges June 1st, 2013 until May 31st, 2015. This time period coincides with when the model was able to assimilate radiosonde observations under its updated resolution and vertical scale. The instruments launched with the twice-daily weather balloons are Vaisala RS92 radiosondes. The pressure, temperature, humidity, and wind sensors are calibrated using Vaisala's CAL-4 calibration machine. Thus, the RS92 serves has as one of the best measurement performances, and GPS technology supporting national upper-air programs. Vaisala reports total uncertainty of 0.5°C for the temperature sensor, 5% for the humidity sensor, 0.15 m/s for wind speed, 2° for wind direction, and 1 hPa for the pressure sensor. The measurement ranges for temperature, humidity, and pressure sensors are -90 to +60°C, 0 to 100%, and 3 to 1080 hPa, respectively (the range for wind observations was not available).

A standard procedure is used for launching the radiosondes, which ensures consistency in the amount of helium used in the balloons and thus in ascent rates. Each individual radiosonde is also calibrated and checked by the ground station equipment technician prior to launch. The sondes are also equilibrated outside prior to launch. Specifically, the instrument is launched at ambient temperature, therefore the instrument needs to equilibrate to its surroundings. The equilibration takes a few minutes and can be monitored by a technician to ascertain that temperature and relative humidity settle to levels matching those from the weather station. For collected data, the quality control procedure screens for physically impossible data. We excluded sondes that were launched at times other than the regular 0 UTC and 12 UTC schedule. For instance, special soundings for atmospheric ozone measurements are sometimes conducted at Summit Station, Greenland at times other than 0 UTC or 12 UTC. Specific variables I will be using are temperature, wind speed and direction, pressure and specific humidity. Any missing data provided by the radiosonde program is indicated as “NAN” in the dataset.

European Centre for Medium-Range Weather Forecasts (ECMWF) Model

I will use output from ECMWF’s operational numerical weather prediction model, the Integrated Forecast System (IFS). The forecasts are performed every twelve hours using a spectral model. The data analyzed by this study are from the 0.5º reduced Gaussian grid with 137 vertical sigma levels. The model grid point nearest to the radiosonde launch location, 72.5°N, 38.5°W, is used here. The model began assimilating radiosonde data from Summit Station in January of 2012; however, on May of 2013, ECMWF updated its sigma levels and resolution to the current 137 vertical levels. Therefore, analysis of the data begins on June 2013 and ends on May of 2015. As for the radiosonde data, the specific variables I will be analyzing are temperature, wind speed and direction, pressure, and specific humidity for all 137 vertical levels.

CHAPTER III

METHODS

Atmospheric variables such as temperature, wind speed, specific humidity, and pressure are available from both the radiosondes and ECMWF model, and will be compared. The observational radiosonde dataset is merged with the model's dataset, to assemble metadata. To determine whether the radiosonde data for a given 0 or 12 UTC timestamp was assimilated into the model, the model output provides a binary variable indicating assimilated versus non-assimilated data. The process of ingesting data into a computer model is referred to as data assimilation. It entails a sequential time-stepping procedure to initialize a forecast with the current state of the atmosphere. Observations from weather stations, radiosondes, satellites, ships, and buoys are assimilated into the model so that that initial conditions in the model most closely resemble the current state of the atmosphere. The model integrates at 12-minute time steps to produce forecasted variables at 3-hour intervals, and assimilates data every 6 hours. The data used in this study include 12-hour and 24-hour forecasts initiated once per day at 12 UTC; each of these times corresponds to the radiosonde launch schedule. Observations available for assimilation may be rejected by the model if they differ significantly from the forecast model first guess. An output of "0" by the model corresponds to a rejection of the assimilated data, while a "1" indicates acceptance. Assimilation rates are calculated from the rejected and accepted output within for each atmospheric variable and layer. The comparison of the mean monthly temperature inversion agreement between the model and the observations is determined by comparing the inversion strength, calculated by subtracting the temperature of the peak of the inversion, from the surface temperature for each day, then taking the mean for the given month.

A statistical analysis is used to evaluate the model drift from the assimilated data throughout the time-step procedure, and to compare the initial state between the model and the observation prior to assimilation. The monthly percentages of radiosondes deployed were calculated to determine the amount of the available data. Also, the percentage of radiosondes that are available for assimilation is calculated. The data were separated into four seasons according to Cox (2015, personal communication): November through March (NDJFM), April and May (AM), June, July, August (JJA), and September and October (SO), as atmospheric and climatological phenomena pertinent to GIS such as temperature inversions and solar irradiance result in differences in the seasonal cycle in the arctic compared with mid-latitudes. The mean and standard deviation of both the model and the radiosonde data are calculated and compared to identify biases in the model for when the radiosonde data is assimilated and when it is not. A t-test is used to determine the significance of the differences between the model with the radiosondes assimilated versus the model without the radiosondes assimilated for each model level for each season. The two-sided Kolmogorov-Smirnov test is applied, as it is suitable for non-parametric distributions. The test calculates whether two independent samples of probability distribution functions (PDFs) are different from each other by comparing the cumulative distribution functions with the null hypothesis that the PDFs are the same. The test is used for the model with the radiosondes assimilated versus the model without the radiosondes assimilated for each model level for each season. Detected differences may be in variance, mean, or shape of the PDFs, but the test does not identify the reason for the detected difference. Finally, p-values are calculated to determine whether or not differences are statistically significant. A significance threshold of 95% is used.

CHAPTER IV

RESULTS

Summit Station Radiosonde Frequency

Figure 1 shows the deployment frequency of the scheduled launches at Summit in each month. With the exception of February of 2011 and July of 2013, all months had approximately 90% or above successfully deployed launches for 0 UTC and 12UTC.

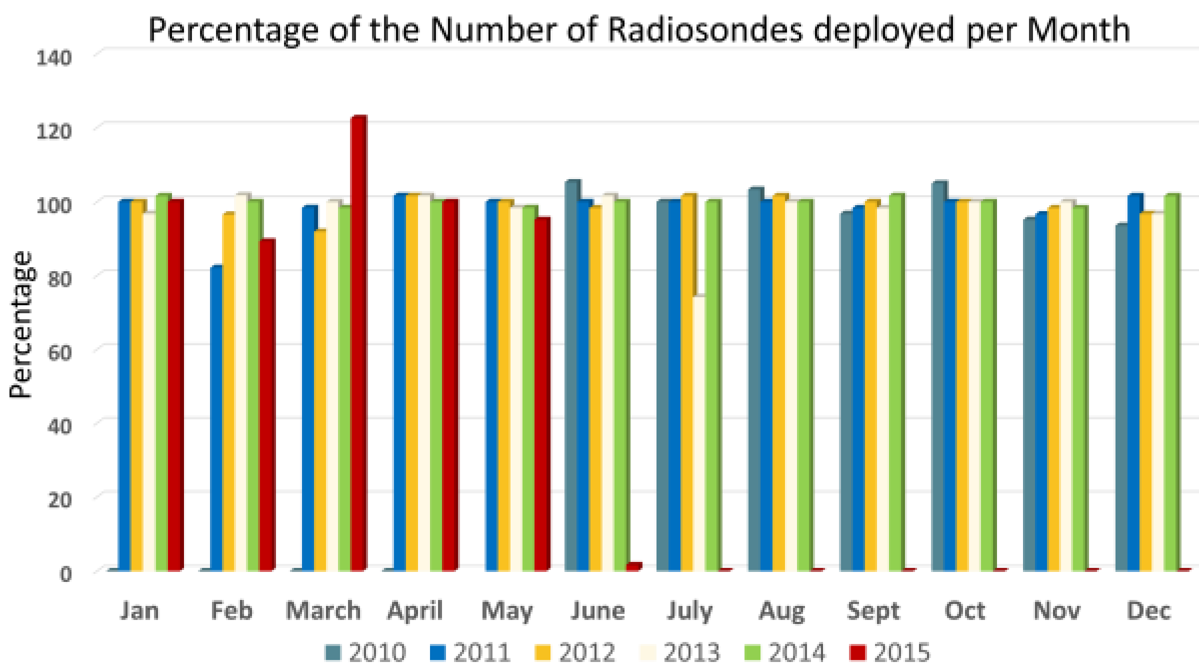

Fig. 1 Frequency of deployed radiosondes in each month from May 2010 through June 2015. Frequencies are calculated assuming two scheduled launches per day.

Reasons for missing launches include equipment failures and high wind conditions (~ > 20 ms^{-1}). As the program began in late May of 2010, the collection of data pertaining to this project begins on June of 2010 and ended at the beginning of June of 2015. There were some months that had above 100% frequency (June, August, and October of 2010), and most notably March of 2015. Occasionally, additional radiosondes are launched at times other than the 0 and 12 UTC schedule, resulting in frequencies above 100% (e.g., March 2015). Overall, the consistent and high percentage of radiosondes deployed at the 0 UTC and 12 UTC timeframes results in a sample-size conducive for comparison with the ECMWF data.

Temperature Inversion Climatology

The subsequent temperature comparison between the ECMWF model (with and without the radiosondes assimilated) and the raw radiosonde observations will be based on inversion strength. Therefore, we first provide a climatology of inversion strength at Summit Station. Climatologically, the greatest inversion strengths occur during the winter months, with a peak in February and a range of 11°C to 12.5°C (Fig. 2). A decline in inversion strength occurs after March and into late spring, with inversion strength decreasing to a minimum of approximately 2.5°C by July. This is followed by a small increase in strength during late summer and into fall. The range from May through August is relatively small, from 2.5°C to 5°C. By September and October, a change in inversion strength is observed, with a mean September of approximately 6°C to 11°C by October.

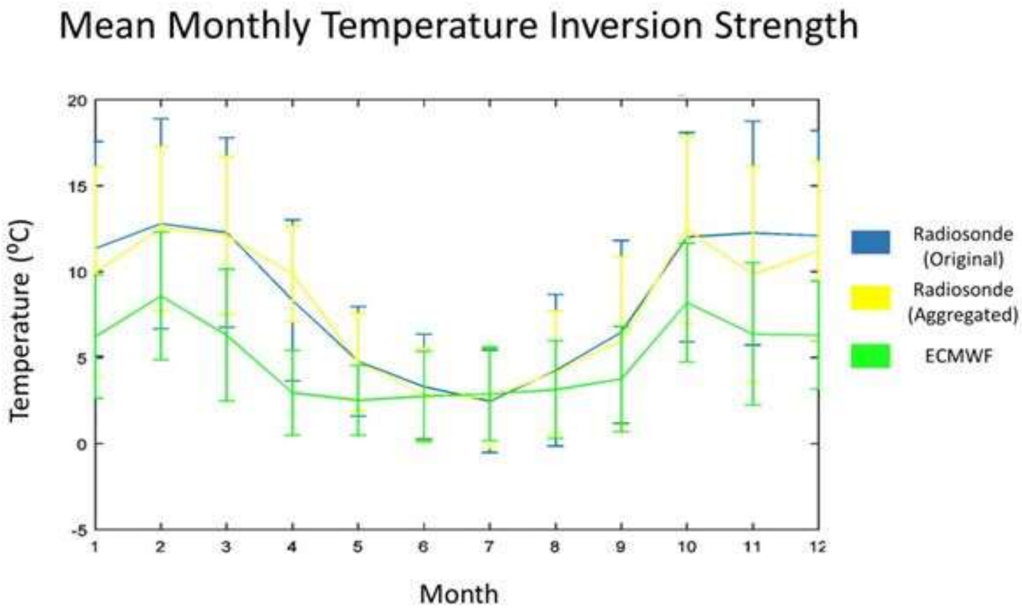

Fig. 2 Mean monthly temperature inversion strength in degrees Celsius. The blue line indicates the original radiosonde data before aggregating to the model. The yellow line is the radiosonde after aggregating to match the vertical resolution of the model. The green line indicates the model with radiosondes assimilated. The whiskers show the variability from the mean.

The radiosonde data resampled to the model elevations shows very similar inversion strengths as the original radiosonde data, suggesting that the model has sufficient resolution to characterize strong inversions. However, ECMWF nonetheless underestimates the inversion during the winter months by 4 – 7°C, and a smaller underestimation during the late spring through early fall with a range from 0.05 – 2.5°C. The aggregation in vertical resolution to match the model had minimal effect on the inversion strength calculated from the radiosonde observations. Therefore, other factors such as the representation of physical processes and/or time step evolution of the model may cause the biases associated with the modeled temperature inversion produced by ECMWF.

ECMWF Radiosonde Assimilation Rates

Assimilation rates for radiosonde temperature varies by season within the boundary layer, corresponding to model levels 138-133 in Fig. 3. Here, a range of 70%-95% is found depending on season. The fall and winter seasons have the lowest assimilation rates in the boundary layer, between approximately 670 hPa to 625 hPa. However, throughout the upper

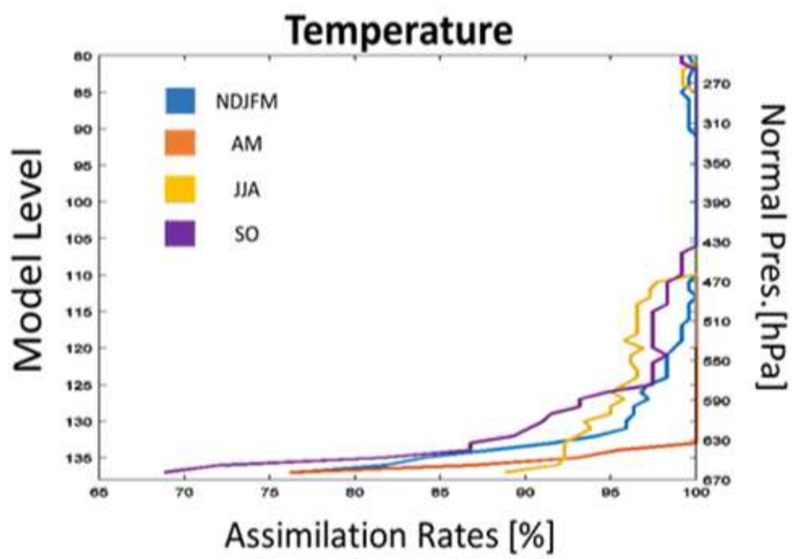

Fig. 3 Assimilated rates of radiosonde temperatures at each model level of ECMWF model level by the Summit Station Radiosonde Program. Model levels are sigma levels with respect to varying surface pressure. For reference, a nominal surface pressure of 670 hPa is used to convert model levels to pressure on the right axis.

levels of the atmosphere, all seasons have assimilation rates at or above 95%. Although the summer is characterized by the highest assimilation rates near the surface, it also has lower assimilation rates than other seasons between the 575 hPa to 470 hPa, although still at or above 95%. Spring experiences the highest assimilation rates above the boundary layer. Given that the temperature inversion strength is greatest during the fall and winter months, a correspondence may exist between the lower assimilation rates of temperature in the boundary layer, an important criterion for inversion strength, and the underestimation of the inversion strength by the model. The model may not be capturing the inversion strength because it is not assimilating the radiosonde data. However, other factors such as the time-step evolution and progression of the model during data assimilation may be at play. The model can reject radiosonde data within the boundary layer as the model goes through the data assimilation process, because the model may find the observations in this layer to be

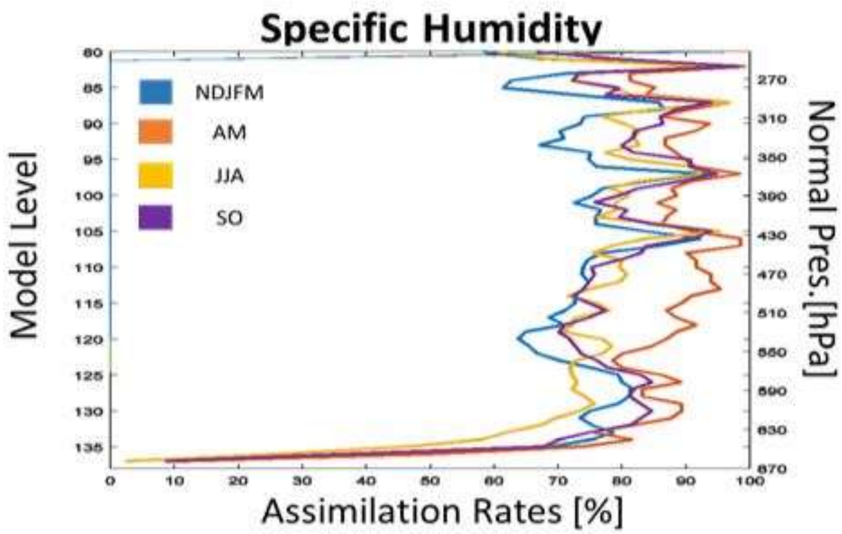

Fig. 4 Assimilated rates of specific humidity at each ECMWF model level. Each model level corresponds to a normalized pressure.

outliers. Some rejections are observed at 310 hPa and above, most likely due to the structure

of the temperature profile associated with the tropopause. The difference in height of the isothermal layer corresponding to the tropopause in the model versus the observations may likely cause the model to reject the data. Less than approximately 60% of the specific humidity observations were assimilated by the ECMWF model between the pressure levels of 670 and 655 hPa (Fig. 4). Below 655 hPa, however, assimilation rates from 60%-90% are found. Summer has the lowest assimilation rates from the surface to approximately 570 hPa.

At the upper-levels, fall, winter, and summer fluctuated from 65% to 95%, whereas spring was less variable with assimilation rates ranging from 80% to approximately 98%. Again, the low assimilation rates within the boundary layer for all season may be a potential explanation for the underestimation of the inversion strength by the model, as specific

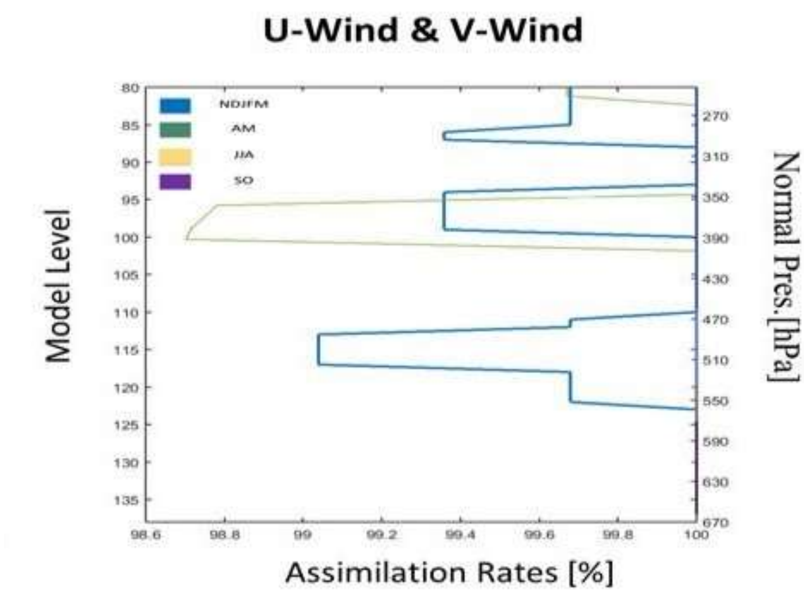

Fig. 5 Assimilated rates of the U and V winds at each ECMWF model level. Each model level corresponds to a normalized pressure.

humidity is also a primary contributor in the variability of the inversion strength.

Interestingly, the U and V components of the winds are, assimilated at rates at or above 98.5% for all levels (Fig. 5). An exact reason for the high assimilation rates is unclear; however, it may because, of all observational products assimilated into the model, radiosondes may be the only observational source of that provides wind data. Therefore, the model may be designed to always this wind data if it is the only available source of the vertical wind fields of the atmosphere over the GIS.

Quantification of ECMWF Radiosonde Assimilation Improvement

Within the boundary layer, from the surface until model level 133, the magnitude of the mean bias decreases between the model without the assimilated temperature radiosonde data versus the model that does assimilate the temperature radiosonde data (Fig. 6, top panel). This is consistent with the model's underrepresentation of inversion strength. Where the inversion itself is located, the boundary layer, the greatest biases associated with

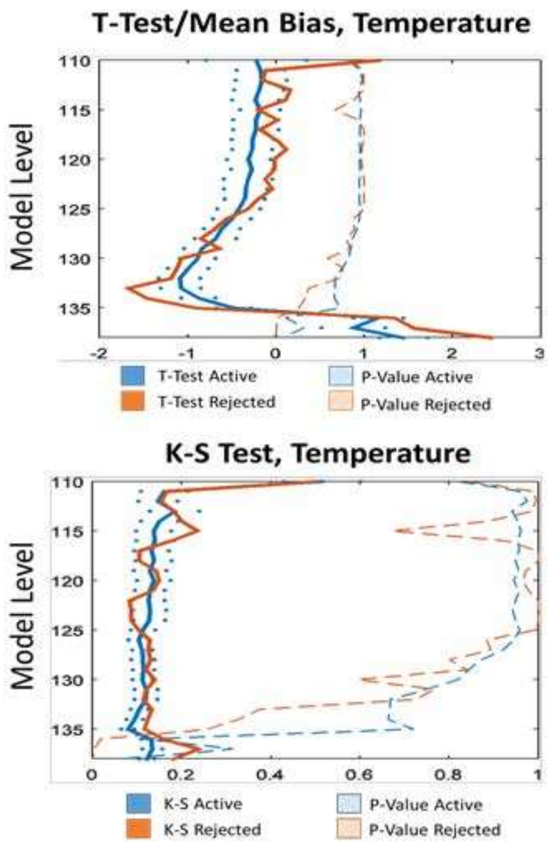

Fig. 6 T-Test (top) and the Kolmogorov-Smirnov test (bottom) for temperature through the boundary- layer and beyond. The solid blue and orange lines indicates the radiosonde data that was assimilated and rejected, respectively by ECMWF. The dashed blue and orange lines are the p-values of the assimilated and rejected data, respectively.

temperature occur. This further suggests a potential relationship between the low temperature assimilation rates in the boundary layer, the high biases in the boundary layer, and the underestimation of the model inversion strength. Overall, the model with the assimilated radiosonde data has a smaller bias than the model without radiosonde assimilation in the boundary layer. The improvement is 0.3-0.7°C near the peak of the negative bias, and near the surface, and the improvement is statistically significant. The improvement may be attributable to the assimilation of observations, but it also may be that the meteorological conditions that occur when radiosondes observation are accepted more closely match the model climatology. Thus the model simulations are consistent with the underestimation shown in Figure 2, and thus further suggests that physical processes in the model cause this bias. Above level 133, there is no detectable bias in either when the model did assimilate the data and when the model did not.

At the boundary layer, the Kolmogorov-Smirnov test statistic is high and indicates statistical significance (Fig. 6, bottom panel). Specifically, the K-S test is higher for the model simulations without the radiosonde observations assimilated than the model simulations with the radiosonde observations assimilated at the surface up until model level 131. Therefore, there is a statistically significant difference between the model assimilating the radiosonde data versus not assimilating the radiosonde data. Above model level 131, up to model level 112, the model assimilating the data versus not assimilating the data are not different, as indicated by the non-significant p-values; therefore, the improvement is inconclusive in terms of when the model assimilated the radiosonde data than when the model did not assimilate the radiosonde data. In addition, given the assimilation rates are at or above 90% above model level 31, there is a very small sample size of simulated temperatures with radiosonde observations rejected, thus it is difficult to definitively

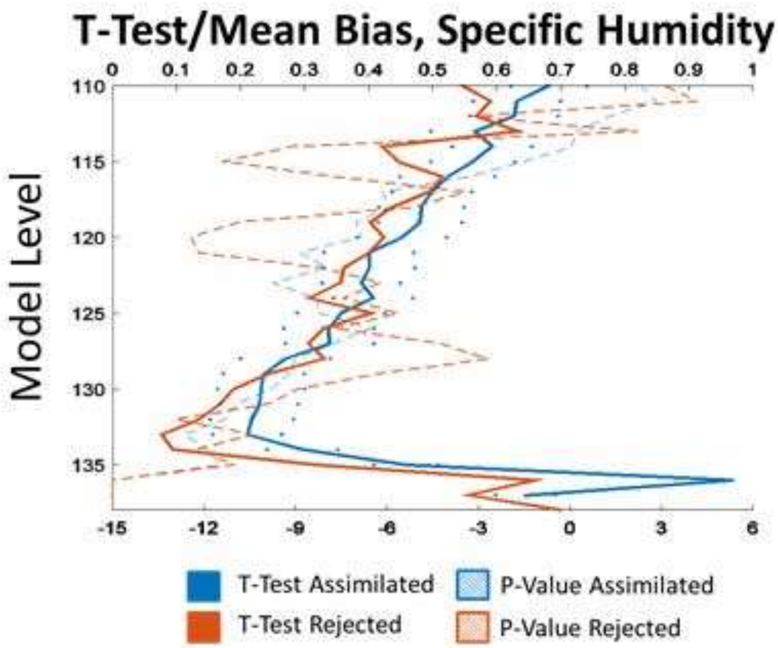

Fig. 7 Similar to Fig. 6 top panel, but for specific humidity.

conclude whether there is an improvement in the levels above level 131. A similar pattern is shown with the mean bias between the model rejecting the specific humidity radiosonde data versus assimilating the specific humidity radiosonde data. However, the model has less of a bias at the surface and from level 135 until model level 128 when the model assimilates the observations than when the model did not assimilate the observations (Fig. 7). Given the small difference between the model humidity with and without radiosonde observations assimilated, there is improvement in the specific humidity at the boundary layer. There is a 0.1 to 0.3 g/kg improvement for assimilated cases. Beyond level 128, similar negative biases exist with the model assimilating the data than when the model did not. The specific humidity difference is therefore inconclusive in regards to the improvement or lack thereof

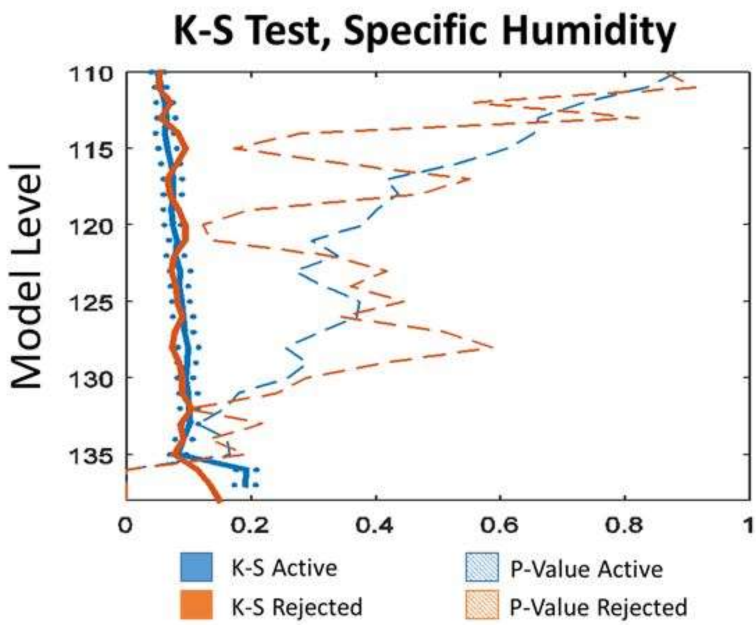

Fig. 8 Similar to Fig. 6 bottom panel, but for specific humidity.

when the model assimilates the radiosonde information. In addition, a caveat on sample size applies within the upper levels: given the small sample size of the model that did not assimilate the observations at the upper levels, it is difficult to definitively assess whether there is improvement at the upper levels of the atmosphere.

At the boundary layer, the Kolmogorov-Smirnov statistic indicates that, from model level 138 to 135, the PDFs are significantly different between the model assimilating the radiosonde specific humidity data and the model rejecting them. However, the difference is lower with the non-assimilated data by ECMWF than the model with the data assimilated.

A statistical analysis for winds was not conducted given the results of the assimilation rates for winds. Because the model assimilated radiosonde observations on all model levels and assimilation rates are at or above 98%, the sample size of model data with rejected radiosonde observations is too small to statistically assess any improvements in the model when the radiosonde data were assimilated.

CHAPTER V

CONCLUSION

We investigated the influence of the Greenland Summit station radiosonde program on biases in the ECMWF (IFS) model. We assessed the radiosonde assimilation rates by ECMWF across all seasons for a 3-year period, established the meteorological regimes that result in lower assimilation, and determined how well the model assimilated radiosonde data at each of the 137 model levels. Next, we quantified the improvement in model forecasts when radiosonde data end up getting assimilated. To do this, a statistical analysis was performed to calculate the biases associated with ECMWF assimilating radiosonde data versus not assimilating. An underestimation of the temperature inversion strength by ECMWF-IFS was found, with a 4-7°C difference during the winter months, and a 0-2.5°C difference during the summer months. Assimilation rates by ECMWF-IFS are higher above the boundary layer for all assessed atmospheric variables, ranging from 85%-100%, 60%-98%, and greater than 98% for temperature, specific humidity, and wind speed, respectively. Thus, specific humidity and temperature are meteorological regimes resulting in the lower assimilation rates likely contributed by a meteorological feature on the in GIS: a shallow temperature inversion. Assimilation of radiosonde observations improves the model forecasts, as biases for both temperature and specific humidity at the boundary layer were reduced by 0.2-0.7°C and 0.1-0.3 g/kg, respectively, and are statistically significant. However, other factors such as meteorological conditions at Greenland and the representation of physical processes in the model may play a role, thus further investigation is warranted. Nevertheless, the temperature inversion over the GIS is a likely the cause of the low assimilation rates within the boundary layer and high biases in both temperature and specific humidity, even with the high assimilation rates for wind. Vertical resolution does not appear to be a factor in the cause of the biases in ECMWF-IFS; i.e., the vertical resolution appears to be sufficient to capture atmospheric features such as the inversions. Rather, the representation of physical processes in the model may be responsible for the underestimation in the inversion strength and further analysis focusing on components of the surface energy budget is recommended. Overall, these findings are significant for the scientific community when investigating the climatological patterns associated with temperature inversions over the GIS and their representation in models. Such patterns as energy and mass exchanges may be better understood with a better representation of the inversion strength in the GIS. Finally, these results signify the importance of accurately characterizing the atmosphere over Greenland and weather prediction and climate. Improvements with models in accurately capturing meteorological regimes such as the shallow temperature inversion can result in improvements in further understanding the climatology of the GIS in addition to enhancing Arctic weather prediction.

REFERENCES

Box E. J., and Steffen K., 2001: Sublimation on the Greenland Ice Sheet from automated weather station observations, *Journal of Geophysical Research*,118, 495–506.

Church, J.A., P.U. Clark, A. Cazenave, J.M. Gregory, S. Jevrejeva, A. Levermann, M.A. Merrifield, G.A. Milne, R.S. Nerem, P.D. Nunn, A.J. Payne, W.T. Pfeffer, D. Stammer and A.S. Unnikrishnan, 2013: Sea Level Change. In: Climate Change 2013: The Physical Science Basis. Contribution of Working Group I to the Fifth Assessment Report of the Intergovernmental Panel on Climate Change [Stocker, T.F., D. Qin, G.-K. Plattner, M. Tignor, S.K. Allen, J. Boschung, A. Nauels, Y. Xia, V. Bex and P.M. Midgley (eds.)]. Cambridge University Press, Cambridge, United Kingdom and New York, NY, USA.

Darby L., T. Uttal, A. Makshtas, and J. Drummond, 2011: International Arctic Systems for Observing the Atmosphere (IASOA). In Understanding Earth's Polar Challenges: *International Polar Year 2007-2008 Summary by the IPY Joint Committee*, eds. I., 391-396.

Fichefet, T., C. Poncin, H. Goosse, P. Huybrechts, I. Janssens, and H. Le Treut, 2003: Implications of changes in freshwater flux from the Greenland ice sheet for the climate of the 21st century. *Geophys. Res. Lett.*, 30(17), 1911.

Ford, J., G. McDowell, J. Jones, 2014: The state of climate change adaptation in the Arctic. *Environ. Res. Lett.* 9 104005

Graversen G. R., 2006: Do Changes in the Midlatitude Circulation Have Any Impact on the Arctic Surface Air Temperature Trend?. *J. Climate*, 19, 5422–5438.

Graversen G. R., T. Mauritsen, M. Tjernström, E. Källén, and G. Svensson, 2008: Vertical structure of recent Arctic warming. *Nature*, 451, 53-56.

Hall, D. K., J. C. Comiso, N. E. DiGirolamo, C. A. Shuman, J. E. Box, and L. S. Koenig, 2013: Variability in the surface temperature and melt extent of the Greenland ice sheet from MODIS, *Geophysical Research Letters*, 40, 1–7.

Hinzman D. L., et al., 2005: Evidence and Implications of recent Climate Change in Northern Alaska and other Arctic Regions. *Climate Change,* 72, 251-298

Maykut G. (1986). The Surface Heat and Mass Balance. *The Geophysics of Sea Ice*. 395-463

Mernild, S. H., and G. E. Liston, 2010: The influence of air temperature inversions on snowmelt and glacier mass balance simulations, Ammassalik Island, Southeast Greenland. *J. Appl. Meteor. Climatol.*, **49**, 47–67.

Miller, N. B., D. D. Turner, R. Bennartz, D. M. Shupe, S. M. Kulie, P.M. Cadeddu, and V. P. Walden 2013: Surface-based inversions above central Greenland, *Journal of Geophysical Research*,118, 495–506.

Overpeck, J., Hughen, K., Hardy, D., Bradley, R., Case, R., Douglas, M., Finney, B., Gajewski, K., Jacoby, G., Jennings, A., Lamoureux, S., Lasca, A., MacDonald, G., Moore, J., Retelle, M., Smith, S., Wolfe, A., and Zielinski, G., 1997: Arctic Environmental Change of the Last Four Centuries', *Science,* 278, 1251-1256.

Serreze C. M., C. R. Schnell, and D. J. Kahl, 1992: Low-Level Temperature Inversions of the Eurasian Arctic and Comparisons with Soviet Drifting Station Data. *J. Climate*, 5, 615–629.

Serreze C. M., E. J. Walsh, S. F. Chaplin III, T. Osterkamp, M. Dyurgerov, V. Romanovsky C. W. Oechel, J. Morison, T. Zhang, and G. R. Barry, 2001: Observational Evidence of Recent Change in the Northern High-Latitude Environment. *Climate Change*, 46, Issue 1-2, 159-207.

Shepherd A., et al., 2012: A Reconciled Estimate of Ice-Sheet Mass Balance, *Science,* 338, 1183-1189.

Smith C. L., V. W. Chu, K. Yang, C. J. Gleason, L. H. Pitcher, A. K. Rennermalm, C. J. Legleiter, A. E. Behar, B. T. Overstreet, S. E. Moustafa, M. Tedesco, R. R. Forster, A. L. LeWinter, D. C. Finnegan, Y. Sheng, and J. Balog, 2015: Efficient meltwater drainage through supraglacial streams and rivers on the southwest Greenland ice sheet. *Proceedings of the National Academy of Science of the United States of America*, 112(4), 1001-1006.

Starkweather S., V. Walden, T. Uttal, J. Drummond, J. Key, J. Kay, T. Vihma, H. Skov, J. Burkhart, 2013: Advancing Arctic Atmospheric Science through Developing Collaborative Targets for Large, International Observatories. *Community White Paper for Arctic Observing Summit 2013.*

Weidick, A., 1995: The Landsat images of Greenland: Satellite Image Atlas of Glaciers of the World: Greenland, edited by: Williams, R. S. and Ferrigno, J. G., United States *Geological Survey Professional Paper* 1386-C.